Available online at www.sciencedirect.com

ScienceDirect

Energy Procedia 64 (2015) 91 – 100

Energy Procedia

3rd Trondheim Gas Technology Conference, TGTC-3

Multiphase flow in complex valve geometry

S. Edvardsen*, C.A. Dorao, O.J. Nydal

Norwegian University of Science and Technology, Kolbjørn Hejes vei 2, 7491 Trondheim, Norway

Abstract

Downhole shut-in valves are used for testing of oil and gas reservoirs. The internal flow geometry is complex, and contains annulus flow, annular contractions, sharp angles, valve ports and sudden expansions. A new procedure for calculating two-phase pressure loss in a downhole shut-in valve is proposed. Flow-pattern independent two-phase flow correlations are here used with a one-dimensional model of the valve in order to simulate two-phase flow. The one-dimensional model is solved using a Least Squares Spectral Element method. Two-phase flow experiments with air/water and air/oil mixtures are performed on a full-scale shut-in valve mock-up. Experimental two-phase flow pressure drop values are then compared to simulations with different correlations. The Müller Steinhagen and Heck correlation is found to be the best choice, giving an average deviation of 12% with the assumption of homogeneous flow.

Peer-review under responsibility of the Scientific Committee of TGTC-3

Keywords: Single phase; Multiphase; Spectral elements; Least squares; Simulation; Validation

1. Introduction

Downhole shut-in valves are used when testing oil and gas reservoirs. Fig.1 shows a typical shut-in valve. The study of the pressure build up curve after a sudden downhole shut-in (closing) of a flowing well provides important information about oil and gas reservoir characteristics, in particular size and near wellbore region. This information is obtained from gauges hanging below the shut-in valve. Traditionally, shut-in operations are performed by operating a valve at the well-head, but errors are introduced in reservoir estimates due to the wellbore storage effect.

* Corresponding author. Tel.: +47 98296939; fax: +47 73593580.
E-mail address: svein.edvardsen@ntnu.no

Peer-review under responsibility of the Scientific Committee of TGTC-3
doi:10.1016/j.egypro.2015.01.012

Nomenclature

A	cross sectional area	(m²)
B	Chisholm B-parameter	
C	Chisholm C-parameter	
f	friction factor, Darcy	
g	acceleration of gravity	(m/s²)
G	mass flux	$(\frac{kg}{m^2 s})$
K	minor loss factor	
$\dot{m}$	mass flow rate	
n	Blasius exponent for friction factor equation	
P	pressure	(Pa)
Δp	pressure drop	(Pa)
v	flow velocity	(m/s)
x	flow quality (gas mass flow / total mass flow)	(-)
X	Lockhart-Martinelli parameter	(-)
z	coordinate along the flow path	(m)

Greec Symbols

α	void fraction	
Γ	physical properties coefficient	
μ	viscosity	$(\frac{N}{m^2 s})$
ρ	density	$(\frac{kg}{m^3})$
τ	shear stress	$(Pa = \frac{N}{m^2})$
$\varphi_{(\ )}$	pressure drop multiplier	(-)

Subscripts

FG	frictional-gas
FG0	frictional, assuming total mass flux as gas
FL	frictional-liquid
FL0	frictional, assuming total mass flux as liquid
G	gas
H	homogeneous
i	inner
L	liquid
Loss	overall loss factor for minor losses
TF	two-phase
Total	sum of liquid and gas
w	wall

Performing a downhole shut-in operation can reduce this source of error. The downhole shut-in valve will however give a pressure drop in the wellbore, and the multiphase flow resistances in a downhole shut-in valve have to be examined theoretically and experimentally in order to improve the analysis of the test results. The value of this pressure drop can also be used as an indicator of the flow across the shut-in valve.

The flow path through the valve-packer assembly is complex, with a series of minor losses as contractions, expansions, sharp angles and obstructions. The first part is annular, between the lower part of the valve and the production tubing. After the valve ports at detail A, Fig.1, there is a chamber, followed by a contraction and a long channel through the packer. The total pressure drop across the valve-packer assembly will here be simulated with a novel one-dimensional finite element method using the least-squares method with spectral element approximation [1].

Similar flow conditions with turbulent multiphase flow can be expected to occur in other parts of subsea oil and gas production systems. One example is the flow through a well plug during pressure equalization before removal of the plug. The flow path through the plug can be compared to a shut-in valve, and knowledge of the flow rate at different pressures is important to avoid problems when operating wire line equipment.

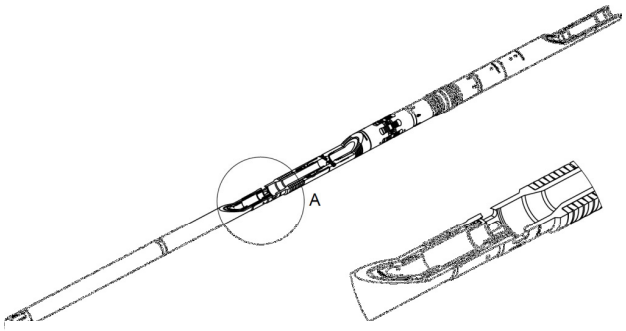

Fig.1. Shut-in valve.

2. Theoretical background

The approach here is to calculate the multiphase pressure drop by using various multiphase flow correlations:

$$\Delta P_{twophase} = \varphi^2 \Delta P_{single\ phase} \tag{1}$$

Many different empirical correlations exist for the multiplier, φ, starting with the classical Lockhart-Martinelli [2] correlations. Here only "black box models", that are flow pattern independent will be evaluated. Finding the two-phase pressure drop will therefore be a two-fold problem: The single-phase pressure drop must be determined as precisely as possible, and then a suitable correlation must be applied. The flow path is too complex to use standard minor loss factors, so the best option for predicting single phase pressure loss is using CFD-simulation on a 3-dimensional model. Edvardsen, et al. [3] have shown that the overall pressure drop can be determined with a CFD-simulation with an error of only 3%. Applying a two-phase multiplier directly to the total single phase pressure loss resulted in a two-phase pressure drop error of 20-30%.

In order to improve the accuracy of the prediction, a 1-D model for single phase compressible and incompressible flow through the valve-packer assembly was established based on the CFD simulations [4]. The frictional and minor losses like contractions, expansions and orifices for this model are given in Table 1.

The two phase flow through the valve can be modeled with the Navier-Stokes Equation. For a 1-dimensional, steady state horizontal flow the following equations can be derived for a slab Δz of the flow:

$$(1-\alpha)\rho_l v_l \frac{\partial v_l}{\partial z}\Delta z + \alpha \rho_g v_g \frac{\partial v_g}{\partial z}\Delta z = -\frac{\partial P}{\partial z}\Delta z - \frac{4}{D_i}\tau_w \Delta z \tag{2}$$

In this momentum balance equation τ_w [Pa] is shear stress at tube wall, α is void fraction and P [Pa] is pressure. The total force from the shear stress τ_w acting along the slab ∂z is here divided by the tube cross section. The resulting pressure drop can also be expressed by the Darcy formula for the case of single phase flow:

$$\Delta P = \rho f \frac{\Delta z}{D} \frac{v^2}{2} = \frac{4\tau_w \pi D \Delta z}{\pi D^2} = \frac{4\tau_w \Delta z}{D} \tag{3}$$

And therefore

$$\tau_w = \rho f \frac{v^2}{8} \tag{4}$$

Pressure drop across singularities are expressed by the minor loss coefficients K from Table 1:

$$\Delta P = \rho K \frac{v^2}{2} = K \frac{G^2}{2\rho} \tag{5}$$

Table 1. Frictional and minor losses in the STC downhole valve.

No.	Description	Length (m)	Minor loss coeff.	Diameter (m)	Hydraulic diameter (m)
1	Circular	0.100		0.0849	0.0849
2	Diffuser, 16°	0.030	0.036	0.0849 < 0.094	
3	Circular, at inlet	0.525		0.094	0.094
4	Annular contraction, 90°	0.015	0.366	0.094 >	0.024
5	Annular	1.259		0.094 x 0.070	0.024
6	Annular contraction, 90°	0.004	0.095		0.024 > 0.020
7	Annular	0.075		0.094 x 0.074	0.02
8	Annular contraction, 90°	0.006	0.071		0.020 > 0.016
9	Annular	0.020		0.094 x 0.078	0.016
10	Valve opening	0.075	1.759		0.016 > 0.060
11	Contraction, 40°	0.030	0	0.060 < 0.040	
12	Circular	0.192		0.04	0.04
13	Equalizing central	0.058	0.284		
14	Circular, through packer	1.220		0.04	0.04
15	Expansion	0.288	0.255	0.040 < 0.090	
16	Circular	0.958		0.09	0.09

For two-phase flow a multiplier is introduced in equation (3). It has been shown [3] that the Müller Steinhagen and Heck correlation [5] and the Chisholm B-correlation [6] gives the best prediction for the overall pressure drop, when applying the two-phase multiplication factor to the total single phase pressure drop. Both correlations will be tested, together with the Friedel correlation. The Chisholm B-correlation is given by:

$$\varphi_{FLo}^2 = 1 + (\Gamma^2 - 1)\left[B x^{(2-n)/2}(1-x)^{(2-n)/2} + x^{2-n}\right] \tag{6}$$

where x is flow quality: $x = \dot{m}_G/(\dot{m}_G + \dot{m}_L)$. The physical coefficient Γ is

$$\Gamma = \frac{\Delta P_{FG0}}{\Delta P_{FL0}} = \left(\frac{\mu_G}{\mu_L}\right)^n \frac{\rho_L}{\rho_G} \tag{7}$$

The meaning of the notation ΔP_{FG0} is the pressure drop assuming total mass flux as gas. Chisholm recommends a B-value of 2.3 for globe valves, and for this valve B is set to 2.5. Then, for two-phase flow the shear stress

$$\tau_w = \rho f_{L0} \frac{v^2}{8} \varphi_{FLo}^2 \tag{8}$$

The Müller, Steinhagen and Heck correlation is given by

$$\left(\frac{dP}{dx}\right)_{TF} = G_{MS}(1-x)^{1/3} + Bx^3 \tag{9}$$

Where $G_{MS} = A + 2(B-A)x$, A = $\left(\frac{dP}{dx}\right)_L = f_L \frac{G_{Total}^2}{2D_i\rho_L}$, $f_L = \frac{0.314}{Re_L^{0.25}}$, $Re_L = \frac{G_{Total}D_i}{\mu_L}$, $B = \left(\frac{dP}{dx}\right)_G = f_G \frac{G_{Total}^2}{2D_i\rho_G}$, $f_G = \frac{0.314}{Re_G^{0.25}}$ and $Re_G = \frac{G_{Total}D_i}{\mu_G}$.

A two-phase multiplier can then be calculated from $\varphi_{FLo}^2 = \left(\frac{dP}{dx}\right)_{TF} / A$ The Friedel correlation [7] is given by

$$\varphi_{FR}^2 = E + \frac{3.24FH}{Fr_H^{0.045} We_L^{0.035}} \tag{10}$$

where $\mathrm{Fr}_H = \frac{G_{total}^2 d_i}{\sigma \rho_H}$, $\mathrm{E} = (1-x)^2 + x^2 \frac{\rho_L f_G}{\rho_G f_L}$, $\mathrm{F} = x^{0.78}(1-x)^{0.224}$, $\mathrm{H} = \left(\frac{\rho_L}{\rho_G}\right)^{0.91} \left(\frac{\mu_G}{\mu_L}\right)^{0.19} \left(1 - \frac{\mu_G}{\mu_L}\right)^{0.7}$ and $We_L = \frac{G_{total}^2}{g d_i \rho_H^2}$.

The two-phase multiplier is only applied to frictional pressure losses. Due to the high turbulence intensity, the phase velocities are believed to be equal. The homogeneous void fraction is then [8]:

$$\alpha = (x\rho_L)/(x\rho_L + (1-x)\rho_G) \tag{11}$$

2.1. Least squares method

The dynamic equation for momentum (Eq. 2) is solved using the least-squares method with spectral element approximation. This method was also used by Ciapero [9] and Sporleder [10]. The use of the least squares method involves the minimization of a norm-equivalent functional. We have that

$$L\mathbf{u} = \mathbf{g} \text{ in } \Omega$$
$$B\mathbf{u} = \mathbf{h} \text{ on } \partial\Omega$$

where Ω and ∂Ω are the domain and the boundary of the domain respectively. *L* is a linear operator and *B* is the trace operator. With the requirement that the system is well-posed and that the operators *L* and *B* being continuous mappings between the function space X(Ω) onto the solution space Y(Ω)×Y(∂Ω) , the norm equivalent functional becomes

$$I(u) = \frac{1}{2}\|L\mathbf{u} - \mathbf{g}\|_{Y(\Omega)}^2 + \frac{1}{2}\|B\mathbf{u} - \mathbf{h}\|_{Y(\partial\Omega)}^2$$

Variational analysis gives

$$\lim_{\epsilon \to 0} \frac{d}{d\epsilon} I(\mathbf{u} + \epsilon \mathbf{v}) = 0 \ \forall \ \mathbf{u} \in \mathrm{X}(\Omega)$$

I can now be minimized with the following necessary condition: Find $\mathbf{u}\in X(\Omega)$ such that

$$A(\mathbf{u},\mathbf{v}) = F(\mathbf{v})\ \forall\ \mathbf{v}\in X(\Omega)$$

and

$$A(\mathbf{u},\mathbf{v}) = \langle L\mathbf{u}, L\mathbf{v}\rangle_{Y(\Omega)} + \langle B\mathbf{u}, B\mathbf{v}\rangle_{Y(\partial\Omega)}$$
$$F(\mathbf{v}) = \langle \mathbf{g}, L\mathbf{v}\rangle_{Y(\Omega)} + \langle \mathbf{h}, B\mathbf{v}\rangle_{Y(\partial\Omega)}$$

$A:X\times X\rightarrow\mathbb{R}$ is a symmetric, continuous bilinear form. $F:X\rightarrow\mathbb{R}$ is a continuous linear form.

2.2. Spectral element formulation

As for finite element formulations, the computational domain Ω is divided into N_e non-overlapping sub-domains Ω_e such that

$$\Omega = \bigcup_{e=1}^{N_e}\Omega_e \ \text{ with } \Omega_e\cap\Omega_k = \emptyset,\ e\neq k$$

The unknown function u_h^e is approximated in each element Ω_e by the set of all polynomials P_Q of degree$\leq Q$. The global approximation u_h in Ω is

$$u_h = \bigcup_{e=1}^{N_e} u_h^e$$

Within each element, the solution is expanded in Φ_i basis functions

$$u_h^e(x) = \sum_{n=0}^{i} u_n^e\Phi_i(\xi)$$

with $(\xi) = X_e^{-1}(x)$ the local coordinate of (x) in the parent element, with $-1\leq\xi\leq1$, and u_h^e the coefficients in the expansion.

2.3. Linearization

The Least-squares method with Spectral Elements requires linear equations, and the term $v\ \partial v/\partial x$ for convective acceleration can be linearized using the Newton-Raphson linearization:

$$u_{k+1} = u_k + \delta u$$
$$u\frac{\partial u}{\partial z} = (u_k+\delta u)\left(\frac{\partial u_k}{\partial z}+\frac{\partial \delta u}{\partial z}\right)$$
$$u\frac{\partial u}{\partial z} = u_k\frac{\partial u_{k+1}}{\partial z} + u_{k+1}\frac{\partial u_k}{\partial z} - u_k\frac{\partial u_k}{\partial z}$$

2.4. Numerical solution

No mass transfer takes place between the phases here, and for elements with a change in cross-section A we have that

$$\frac{\partial u}{\partial z} = \frac{\partial u}{\partial A}\frac{\partial A}{\partial z} = \frac{\partial}{\partial A}\left(\frac{\dot m}{A\rho}\right)\frac{\partial A}{\partial z} \quad\text{and}\quad \frac{\partial u}{\partial z} = -\left(\frac{\dot m}{A^2\rho}\right)\frac{\Delta A}{\Delta z}$$

The differential equation $L\mathbf{u} = \mathbf{g}$ can now be written as follows for multiphase flow:

$$\begin{Bmatrix} \frac{\partial}{\partial z} & 0 & 0 \\ 0 & \frac{\partial}{\partial z} & 0 \\ v_G^* \frac{\partial}{\partial z} + \frac{\partial v_G^*}{\partial z} & v_L^* \frac{\partial}{\partial z} + \frac{\partial v_L^*}{\partial z} & \frac{\partial}{\partial z} \end{Bmatrix} \begin{Bmatrix} \alpha \rho_G v_G \\ (1-\alpha)\rho_L v_L \\ P \end{Bmatrix} = \begin{Bmatrix} -\left(\frac{\dot{m}_G}{A^2}\right)\frac{\partial A}{\partial z} \\ -\left(\frac{\dot{m}_L}{A^2}\right)\frac{\partial A}{\partial z} \\ -\varphi^2 \frac{4}{D_i}\tau_w - v_G^*\left(\frac{\dot{m}_G}{A^2}\right)\frac{\partial A}{\partial z} - v_L^*\left(\frac{\dot{m}_L}{A^2}\right)\frac{\partial A}{\partial z} \end{Bmatrix} \quad (12)$$

The superscript asterisk indicates that this is a value from the previous iteration. If the element has a minor loss factor, the right side is

$$\begin{Bmatrix} \frac{\partial}{\partial z} & 0 & 0 \\ 0 & \frac{\partial}{\partial z} & 0 \\ v_G^* \frac{\partial}{\partial z} + \frac{\partial v_G^*}{\partial z} & v_L^* \frac{\partial}{\partial z} + \frac{\partial v_L^*}{\partial z} & \frac{\partial}{\partial z} \end{Bmatrix} \begin{Bmatrix} \alpha \rho_G v_G \\ (1-\alpha)\rho_L v_L \\ P \end{Bmatrix} = \begin{Bmatrix} -\left(\frac{\dot{m}_G}{A^2}\right)\frac{\partial A}{\partial z} \\ -\left(\frac{\dot{m}_L}{A^2}\right)\frac{\partial A}{\partial z} \\ -K\frac{G^2{}_{Total}}{2\rho_L} - v_G^*\left(\frac{\dot{m}_G}{A^2}\right)\frac{\partial A}{\partial z} - v_L^*\left(\frac{\dot{m}_L}{A^2}\right)\frac{\partial A}{\partial z} \end{Bmatrix} \quad (13)$$

The term $\partial A/\partial z \approx \Delta A/\Delta x$ can be found from geometrical relationships, as all cross section changes are simplified to conical contractions or conical expansions.

3. Experimental setup and testing procedure

A full-scale model of a shut-in valve was installed in the multiphase test loop at NTNU, see Fig. 2.

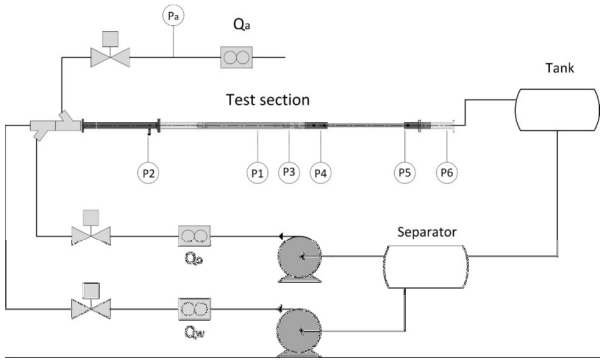

Fig. 2. Valve model in multiphase test loop

The separator allows for continuous circulation of a multiphase flow. The test section has pressure sensors at six different locations, in order to identify the pressure drop as detailed as possible, see Fig. 2. For the total pressure loss the resulting combined accuracy is ±1.3kPa. The dimensions of the valve mock-up are shown in Fig. 3, and experimental conditions are given in Table 2. Flow meter and sensor specifications are given in Table 3.

Table 2. Experimental conditions, 20°C

Fluid	Flow range	Density	Viscosity
Air	0-0.27 kg/s with water / 0-0.02 kg/s with oil	1.2 kg/m^3 at 1 bar	1.8E-5 Pa-s
Water	0-10 kg/s	998 kg/m^3	0.001 Pa-s
Oil, Exxsol D80	0-10 kg/s	798 kg/m^3	0.0018 Pa-s

Table 3. Flow meters and sensors

Flow meter / sensor	Type	Range	Uncertainty	Repeatability
Air, small	Coriolis	0-0.0222 kg/s	±0.1% of	
Air, large	Vortex	0.004- 0.110 m³/s	±1% of rate	±0.25% of
Water	Electromagnetic	0-10 kg/s	±0.5%	±0.15% of
Oil	Coriolis	0-10 kg/s	±0.15% of	
P1-P3	Piezoresistant	0-600 kPa	±0.2%	0.05%
P4-P6	Piezoresistant	-100 to +100 kPa	±0.2%	0.05%

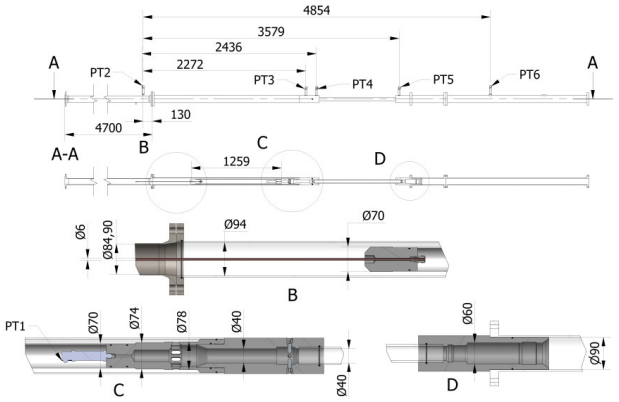

Fig. 3. Shut-in valve mock-up

4. Results and discussion

The numerical simulation of two-phase flow was performed using element lengths approximately equal to the local diameter, totally 76 elements of order 5. Smaller elements did not improve the accuracy. The atmospheric outlet pressure was used as boundary condition, and element pressures were calculated by solving Eq. (12) for elements with frictional pressure drop, or Eq. (13) for elements with a minor loss coefficient. Pressures were calculated for one element at a time, counter current to fluid flow. Air density was updated at each element. The one-dimensional mesh was based on Table 1. The above given correlations for multiphase flow were tested one by one by simulating the full range of flow conditions given in Table 2. The minor losses were calculated as if total mass flow was liquid, without multiphase multiplier. Two-phase air-water and air-oil flow experiments were also performed with the same range of flow conditions.

In order to compare simulated and experimental results, overall multiphase multiplication factors $\varphi_{overall\_corr}$ were calculated for each correlation by dividing simulated total multiphase pressure drop $\Delta P_{TF\_simulated}$ with total experimental liquid flow pressure drop $\Delta P_{L\_experimental}$.

$$\varphi_{overall\_corr} = \frac{\Delta P_{TF\_simulated}}{\Delta P_{L\_experimental}} \tag{14}$$

The corresponding experimental overall multiphase multiplication factors $\varphi_{overall\_exp}$ were calculated from the experimental two-phase pressure drop $\Delta P_{TF\_experimental}$:

$$\varphi_{overall\_exp} = \frac{\Delta P_{TF\_experimental}}{\Delta P_{L\_experimental}} \tag{15}$$

The overall multiphase multiplication factors $\varphi_{overall\_corr}$ will consequently also contain a small deviation from single phase liquid flow pressure drop simulation, which is about -1.2% [4]. The deviations for the for air-water flow simulation results are given in Table 4. Average deviation E_1 and standard deviation E_3 are defined as

$$E_1 = \left[\frac{1}{n}\sum_{i=1}^{n}\frac{\varphi_{overall\_corr(i)}-\varphi_{overall\_\exp(i)}}{\varphi_{overall\_\exp(i)}}\right] \text{ and } E_3 = \sqrt{\frac{1}{n}\sum_{i=1}^{n}\left\{\left[\frac{\varphi_{overall\_corr(i)}-\varphi_{overall\_\exp(i)}}{\varphi_{overall\_\exp(i)}}\right]-E_1\right\}^2}$$

Experimental and simulation results are plotted as function of flow quality $x = \dot{m}_G/(\dot{m}_G + \dot{m}_L)$ in Fig. 4. The overall multiphase pressure drop multiplier $\varphi_{overall}$ is the ordinate in Fig. 4 and 5. The Müller Steinhagen and Heck correlation gives simulation results that are closest to the experimental values, as the error analysis in Table 4 shows only 10.5% average deviation.

Table 4. Air-water flow error analysis.

Correlation	Friedel	Chisholm B	Müller Steinhagen and Heck
Average deviation E_1	22.5%	27.1%	10.5%
Standard deviation E_3	17.3%	19.4%	13.9%

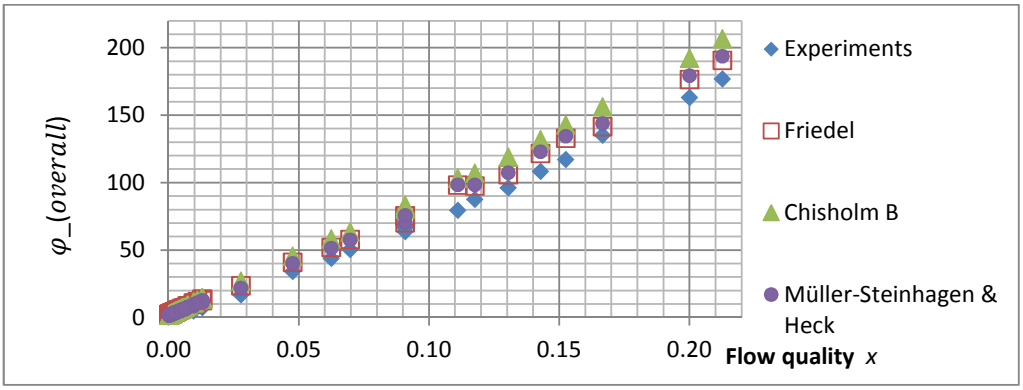

Fig. 4. Air-water flow in shut-in valve mock-up

Results for air-oil flow are given in Fig. 5, and error analysis is given in Table 5. Here the trend is the same, showing that the Müller Steinhagen and Heck correlation gives the best results, with only 12.1% average deviation.

Table 5. Air-oil flow error analysis.

Correlation	Friedel	Chisholm B	Müller Steinhagen and Heck
Average deviation E_1	29.3%	29.6%	12.1%
Standard deviation E_3	35.4%	32.1%	26.3%

5. Conclusions

In this work, a one-dimensional least squares spectral element method was used for predicting the two-phase flow pressure drop in a downhole shut-in valve. The one-dimensional mesh, with 76 elements of order 5, was based on a formerly qualified model for liquid flow [4]. With the outlet pressure as boundary condition, element pressure drops were calculated one by one countercurrent to fluid flow. Two-phase pressure drop was calculated as a product of single phase liquid flow pressure drop and a multiphase flow multiplier. Minor pressure losses were calculated as if total mass flow was liquid. The total pressure drop was determined with only 10.5-12% average deviation compared to experimental values, using the Müller, Steinhagen and Heck correlation for the two-phase multiplier with void fraction calculated for equal phase velocities.

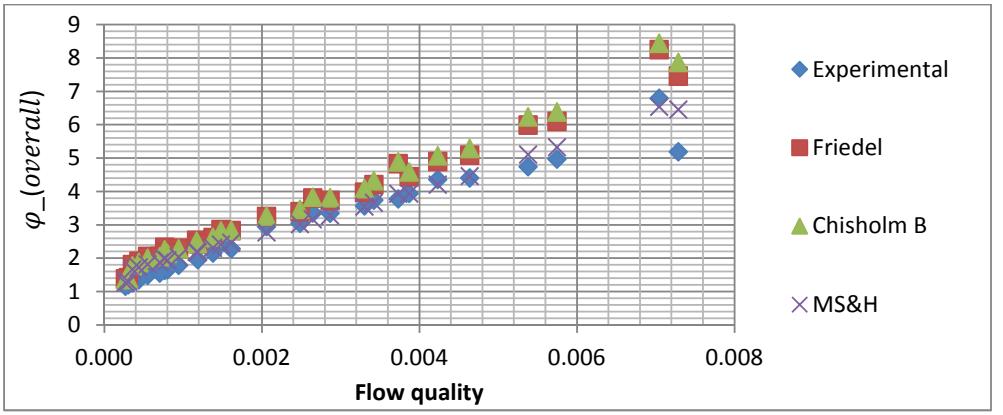

Fig. 5. Air-oil flow tests

References

[1] Proot M, Gerritsma M. Least-squares spectral eelement applied to the Stokes problem. *Journal of Comp. Phys.* 2002; 181(2): 454-477

[2] Lockhart R, Martinelli R. Proposed correlation of data for isothermal two-phase two-component flow in pipes. *Chem. Engn. Progr* 1949; 45(1): 39-48

[3] Edvardsen S, Dorao C, Nydal OJ. Two-phase flow in a down-hole shut-in valve. *9th North American Multiphase Technology Conference*. 2014 June 11-13. Banff, Canada

[4] Edvardsen S, Dorao C, Nydal OJ. Single-phase flow in downhole shut-in valve. 2014: Submitted

[5] Müller-Steinhagen H, Heck K. A Simple Friction Pressure Drop Correlation for Two-Phase Flow in Pipes. *Chem. Engn. Progr* 1986;20: 297-308

[6] Chisholm D. *Two-phase flow in pipelines and heat exchangers*. London: George Godwin; 1983.

[7] Friedel L. Improved Friction Pressure Drop Correlations for Horizontal and Vertical Two-Phase Pipe Flow. *European Two-Phase Flow Group Meeting, Ispra, Italy* 1979 June

[8] Thome J. *Engineering Data Book III*, Lausanne: Swiss Federal Institute of Technology Lausanne; 2010.

[9] Chiapero EM. *Two-phase flow instabilities and flow mal-distribution in parallel channels*. PhD Thesis, Trondheim: Norwegian University of Science and Technology; 2013.

[10] Sporleder F. *Simulation of Chemical Reactors using the Least-Squares Spectral Element method*. PhD Thesis, Trondheim: Norwegian University of Science and Technology; 2011.